Nuclear fusion: Fast heating scalable to laser fusion ignition

Article *in* Nature · August 2002

DOI: 10.1038/418933a

25 authors, including:

Shigekazu Fujioka
Osaka Health Science University
93 PUBLICATIONS **831** CITATIONS
SEE PROFILE

Kunioki Mima
Graduate School for the Creation of New Pho…
906 PUBLICATIONS **13,146** CITATIONS
SEE PROFILE

Kengo Nagai
Osaka Medical Center for Cancer and Cardiov…
215 PUBLICATIONS **3,043** CITATIONS
SEE PROFILE

Ahmed Youssef
Osaka University
22 PUBLICATIONS **429** CITATIONS
SEE PROFILE

Neutron production in ultraintense laser interactions with carbon-deuterated plasma at intensities of 10^{18} W cm^{-2}

2010 Nucl. Fusion 50 035010

(http://iopscience.iop.org/0029-5515/50/3/035010)

IOP Publishing and International Atomic Energy Agency Nuclear Fusion
Nucl. Fusion **50** (2010) 035010 (6pp) doi:10.1088/0029-5515/50/3/035010

Neutron production in ultraintense laser interactions with carbon-deuterated plasma at intensities of 10^{18} W cm^{-2}

A. Youssef[1,a] **and R. Kodama**[2,3]

[1] Physics Department, Faculty of Science, Sohag University, Sohag 82524, Egypt
[2] Graduate School of Engineering, Osaka University, 2-1 Suita, Osaka 565-0871, Japan
[3] Institute of Laser Engineering (ILE), Osaka University, 2-6 Suita, Osaka 565-0871, Japan

E-mail: aeltabal@yahoo.com and ahmed.mohamed9@science.sohag.edu.eg

Received 20 October 2009, accepted for publication 15 February 2010
Published 5 March 2010
Online at stacks.iop.org/NF/50/035010

Abstract
Wide-range neutron energy spectra that are produced when an ultraintense laser with an intensity of 3×10^{18} W cm^{-2} is focused on a CD2 target have been studied. The experimentally observed spectra and numerically calculated ones, by a three-dimensional Monte Carlo code, indicate that the energy range of the emitted neutrons is larger than that of the D(d,n)^{3}He reaction. The reactions that can participate in neutron production and their relative importance have been analysed. An explanation for the measured spectra is introduced by taking into account the ^{12}C(d,n)^{13}N and D(^{12}c,n)^{13}N reactions. These reactions strongly participate in neutron production due to their high cross sections. Moreover, the neutrons from these reactions will overlap the neutrons from the D(d,n)^{3}He reaction, including the 2.45 MeV neutrons, with increasing energy of the accelerated ions under higher irradiances.

PACS number: 52.57.Kk

1. Introduction

The rapid development of ultraintense laser technology has recently sparked enormous scientific activity. Laser systems using the technique of chirped pulse amplification (CPA) allowed focusing a laser to irradiances greater than 10^{20} W cm^{-2} in pico-second pulses containing up to several hundred Joules [1]. Ultraintense laser–plasma interaction represents a very rich area for coupling the fundamental physics and technological progress particularly in fast ignitors of laser fusion [2], medicine [3, 4], material science [5], accelerator technology [6] and tabletop nuclear physics [7]. Once the laser intensity exceeds 10^{18} W cm^{-2}, the generated hot electrons become relativistic, where the average kinetic energy of the electron oscillating in the laser field becomes equivalent to the particle's rest mass and the quiver velocity becomes very close to the speed of light. The propagation of this intense electron beam inside the target generates γ-rays and accelerates ions. The energies of the accelerated ions and the generated photons are sufficient to induce nuclear reactions. These reactions have therefore become very interesting as a diagnostic tool for high-density plasma. Nuclear reactions that produce neutrons are unique probes. Because of their large mean free path and their neutral charge, neutrons readily carry information from inside the target without any effect due to electric and/or magnetic fields inside or around the target. While a relatively large number of studies have focused on measuring hot electrons, γ-rays and emitted ions, studies of the generated neutrons in ultraintense laser–plasma interactions are very rare. In previous works [8–10], we started a series of studies, both experimentally and theoretically, using neutron spectroscopy to investigate some important aspects in laser–plasma interactions.

Experimentally, neutron production by irradiating solid targets with ultra-short lasers at different intensities has been observed [11–18], but identifying the neutron source(s) was not complete. Usually, the D(d,n)^{3}He reaction has been considered the only source of the emitted neutron spectra. However, neutrons with energies lower than 1.63 MeV (the absolute minimum energy of the D–D neutrons) were observed when solid CD2 targets were irradiated by lasers with intensities of the order of 10^{18} W cm^{-2} [12, 17]. Therefore, further detailed investigations are needed to identify the reactions that generate the observed neutrons. Such identification is of critical importance for the experiments of inertial confinement fusion (ICF) in which the measured neutron yield is usually attributed to the D–D reaction only.

[a] Author to whom any correspondence should be addressed.

To identify the neutron producing reactions, an analysis of the emitted neutron energy spectra is necessary. In this context, neutron spectroscopy represents a key element. It is the most detailed probe to distinguish the emitted neutron spectra and their producing reactions. Nuclear reactions occur between accelerated and background ions inside the target so that they can disclose the energy spectrum of the accelerated ions. If these reactions are neutron producing ones, the energy spectrum of the emitted neutrons will provide us with valuable information about the energy spectrum of the accelerated ions. Then the neutron energy range of each reaction caused by these accelerated ions can be recognized. The cross section and the threshold energy of each reaction will reveal its relative importance comparing with the others. Thus, the neutron source(s) can be disclosed. In this paper, we introduce for the first time an analytical study of detailed neutron energy spectra observed when an ultraintense laser with an intensity of $3 \times 10^{18}\,\mathrm{W\,cm^{-1}}$ was focused on CD2 targets in order to identify the emitted neutron spectra and their producing reactions.

2. Experimental work

The 30 TW Gekko MII short pulse laser system [19] at the Institute of Laser Engineering (ILE), Osaka University, was used to perform the experimental part of this work. The 450 fs, 20 J, 1053 nm laser was focused on a CD2 target at an intensity of $3 \times 10^{18}\,\mathrm{W\,cm^{-2}}$. The incident angle of the p-polarized laser light was 20° relative to the target normal. Neutron spectra were detected with neutron spectrometers that consisted of current mode time of flight (TOF) detectors comprising a scintillator/photomultiplier tube (PMT) combination. Two neutron detectors were positioned at 2.17 m and 1.98 m from the target at angles 20° and 70° relative to the target normal, respectively. The scintillator type, ultra-fast timing plastic scintillator, is the quenched version of the Bicron BC-422 scintillator (BC-422Q) with a decay time of 700 ps and a rise time of less than 20 ps [20]. The PMT, one of the highest performance timing tubes, is the Hamamatsu R2083 that has a rise time of 700 ps and a transit time spread of 370 ps.

The detectors were shielded with a 10 cm thick Pb wall placed in front of the scintillator. In addition, detectors were protected by 5 cm of Pb plates on all sides. The modulation of the neutron spectra due to the shielding [21] was taken into account. Therefore, TOF values of the neutron groups were corrected by considering the delay of the neutrons inside the lead blocks. The signal levels were normalized to be the neutron yield per unit solid angle $\mathrm{d}^2N/\mathrm{d}\Omega\,\mathrm{d}E$ (neutrons $\mathrm{MeV^{-1}\,sr^{-1}}$), taking into account the detector position and sensitivity. The accuracy of each energy value was calculated by using the differentiation method [22]. According to this method, the error in neutron energy ΔE is calculated using the partial differentiation depending on the experimental errors in both TOF ΔT and distance of the detector from the target ΔX as

$$(\Delta E)^2 = (\partial E/\partial T)^2(\Delta T)^2 + (\partial E/\partial X)^2(\Delta X)^2.$$

To reduce the effect of the bremsstrahlung flashes, coming from the relativistic electrons interactions with both the instruments close to the target and the chamber wall, cone shaped collimators were installed in the chamber at the observation angles. The collimators limit the view of the detectors and reduce the bremsstrahlung flashes from the diagonal inner walls of the chamber. The body of the collimator is made of a 1 cm thick lead cylinder. To reduce bremsstrahlung on the collimator itself, the lead collimator was covered with a 4.5 cm thick low-z (plastic) electron moderator. The neutron detectors observe the target through a hole bored through the centre of the electron moderator. Therefore, this low-z electron moderator also works as a neutron collimator. To overcome the noises due to Poisson statistics in the measured neutron spectra, the experimental data have been binned with bin length 75 keV.

3. Discussion

When the ultraintense lasers interact with deuterated targets, we can expect the acceleration of the deuterium ions which reflects itself in the reaction D + D → ^{3}He + n + 3.27 MeV. This D–D reaction occurs between accelerated and target background deuterium ions. Such a positive Q value reaction ($Q = 3.27$ MeV) is probable even if the total kinetic energy of the two interacting ions is just enough to overcome the Coulomb barrier. Then, at the moment of the nuclear reaction, the kinetic energy of the interacting deuterons is equal to zero. If so, the released energy of the reaction will be 3.27 MeV (Q value) and the products of the reaction have to have equal and opposite momenta because the initial momentum is zero. As a consequence, the released energy distributes between the outgoing particles in inverse proportion to their masses to conserve the linear momentum. In this case, the reaction can be written as D + D → ^{3}He (0.82 MeV) + n (2.45 MeV) because the emitted neutrons in all the directions carry only one value of energy, that is 2.45 MeV, and the recoil ^{3}He nuclei in the opposite directions have only one value of energy, that is 0.82 MeV. However with increasing total kinetic energy of the interacting deuterons, the released energy will increase by the same amount. The sum of the energies of the outgoing particles will increase by the same amount also. Now, the linear momentum is not equal to zero so that the emitted neutrons in the forward direction will carry higher energies than 2.45 MeV. Besides, neutrons with energies lower than 2.45 MeV will be produced in the backward directions. In all cases, for the forward and backward directions, the energies of the emitted neutrons at a given incident ion energy will be determined by the emission angle θ that is determined by linear momentum conservation.

Figures 1 and 2 show the emitted neutron spectra observed from two angles of observation, 20° and 70° relative to the target normal, when a 5 μm CD2 target is irradiated by an ultraintense laser at an intensity of $3 \times 10^{18}\,\mathrm{W\,cm^{-2}}$. The neutron spectra observed at 20° extend from 75 ± 5 keV up to 4.5 ± 0.31 MeV (figure 1), and those observed at 70° extend from 20 ± 1.4 keV up to 4.0 ± 0.28 MeV (figure 2). This means that the energy range of the measured neutrons extends from 20 ± 1.4 keV up to 4.5 ± 0.31 MeV. The laboratory energy of the emitted neutron E_b as a function of the incident ion energy E_a and the angle θ between the incident ion and the

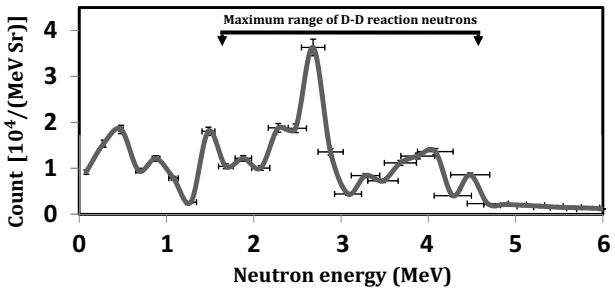

Figure 1. The measured neutron spectra observed at 20°. The spectra extend from 75 ± 5 keV to 4.5 ± 0.31 MeV. The two arrows display the maximum energy range of the D–D reaction neutrons.

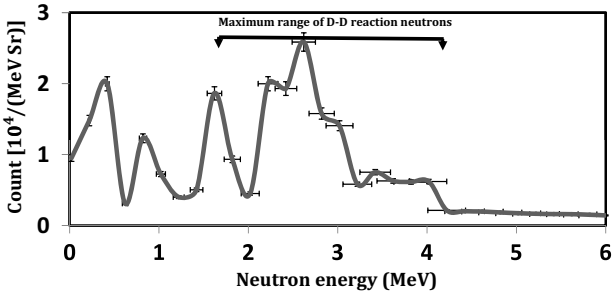

Figure 2. The measured neutron spectra observed at 70°. The spectra extend from 20 ± 1.4 keV to 4.0 ± 0.28 MeV. The two arrows display the maximum energy range of the D–D reaction neutrons.

emitted neutron [23] is given as

$$E_b^{1/2} = ((m_a m_b E_a)^{1/2}\cos\theta \pm \{m_a m_b E_a \cos^2\theta + (m_Y + m_b)[m_Y Q + (m_Y - m_a)E_a]\}^{1/2})/(m_Y + m_b), \quad (1)$$

where m_a, m_b and m_Y are the masses of incident ion, emitted neutron and produced nucleus, respectively. From this formula, the maximum energy of the emitted neutrons (when $\theta = 0°$) will be 4.5 ± 0.31 MeV if the maximum energy of the incident D ions is 1.3 ± 0.22 MeV. This means that, in our case, D ions are accelerated up to 1.3 ± 0.22 MeV and in the same time the minimum energy of the D–D reaction neutrons (when $\theta = 180°$) is 1.7 ± 0.12 MeV. Hence the maximum energy range of the neutron spectra produced by the D–D reaction extends from 1.7 ± 0.12 MeV up to 4.5 ± 0.31 MeV (the arrows in figures 1 and 2 display the maximum range for each observation angle). However, the measured neutron spectra include neutrons with lower energies to 20 ± 1.4 keV. Consequently, the observed spectra cannot be explained by considering the D–D reaction only.

3.1. The Monte Carlo code

To elucidate the observed spectra, we performed numerical experiments by using a three-dimensional (3D) Monte Carlo code. This code is used to calculate the spectra of neutrons produced by the D–D reaction in a finite thickness target and emitted in specific directions of observation. In the code, the incident ions start from a point on the target surface and propagate into the bulk of the target. For the best fitting to the experimental results, ions are assumed to be accelerated in the target normal direction [16] with Maxwellian energy distribution. This means that, in the 3D momentum space, the momentum component of the accelerated ions in the target normal direction is higher than the other components in the directions of the target length and width. The multiple scattering of the accelerated ions inside the target due to small angle scattering by collisions with nuclei and their associated electrons is calculated by using the Jackson equation [24]. The effect of this scattering on the path of the accelerated ions must be small but it is taken into account for the sake of a high degree of accuracy. Neutron yield $Y(\theta)$ emitted in a specific angle θ is calculated through the formula

$$Y(\theta) = \int n_1 n_2 \sigma(E,\theta)\upsilon \, \mathrm{d}t \, \mathrm{d}\upsilon, \quad (2)$$

where n_1 is the number density of the accelerated ions, n_2 is the number of the target ions per unit volume, $\sigma(E,\theta)$ is the differential cross section of the nuclear reaction for a given energy E and an emission angle θ and υ is the velocity of the accelerated ions. The neutron yield is calculated to be the number of neutrons per unit solid angle $\mathrm{d}^2N/\mathrm{d}\Omega\,\mathrm{d}E$ (neutrons $\mathrm{MeV}^{-1}\,\mathrm{sr}^{-1}$). The time step, in the calculations, was taken to be enough for a large number of collisions and the stopping power was taken into account. The differential cross section $\sigma(E,\theta)$ for a given energy E and an emission angle θ is calculated from experimental data and the best fitting calculated values [25] by using Legendre polynomials as follows:

$$\sigma(E,\theta) = \sigma(E,0)\sum A_i P_i(\theta), \quad (3)$$

where $\sigma(E,0)$ is the differential cross section for a given energy E and zero emission angle, P_i are Legendre coefficients and A_i are constants provided that $\sum A_i = 1$. The Monte Carlo code has been run with a large enough sample size to reduce the fluctuations in the calculated spectra. The experimental data and Monte Carlo code output were usefully binned to reduce fluctuations.

The 3D Monte Carlo simulation pointed out that the neutron spectra of the D–D reaction are those observed in the energy range 2.3 ± 0.16–4.5 ± 0.31 MeV at 20° and in the energy range 2.1 ± 0.14–4 ± 0.28 MeV at 70° (figures 3 and 4). To identify the source(s) of the neutron spectra that have lower energies, the other possible neutron producing reactions have to be investigated. These reactions include many processes as follows:

(1) *Deuteron break-up*:

$$\mathrm{D} + \mathrm{D} \rightarrow \mathrm{D} + \mathrm{P} + \mathrm{n} - 2.225\,\mathrm{MeV},$$

$$E_{\mathrm{th}}\,(\text{threshold energy}) = 4.45\,\mathrm{MeV}.$$

The break-up mechanism means the dissociation of an incident deuteron into proton and neutron on the nuclear and/or the Coulomb field of another one. The minimum kinetic energy of the incident deuteron has to be 4.45 MeV. In this work, the maximum acceleration energy of D ions is 1.3 ± 0.27 MeV and as a consequence this reaction is impossible.

(2) *Deuteron electro-disintegration*:

$$\mathrm{e} + \mathrm{D} \rightarrow \mathrm{e} + \mathrm{p} + \mathrm{n} - 2.225\,\mathrm{MeV}, \qquad E_{\mathrm{th}} = 2.225\,\mathrm{MeV}.$$

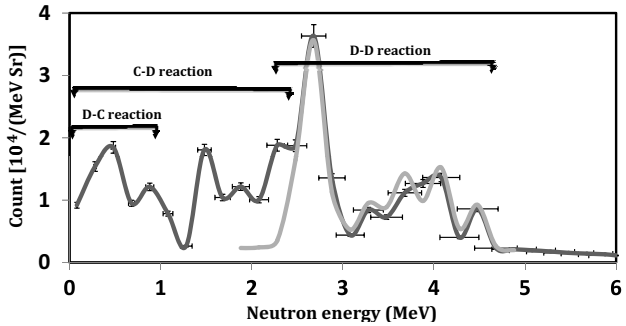

Figure 3. Comparison between the measured neutron spectra (black) and the calculated spectra for the D–D reaction by 3D Monte Carlo code (grey) at observation angle 20°. The D–D reaction can introduce an acceptable interpretation for the measured neutron spectra from 2.3 ± 0.16 MeV to 4.5 ± 0.31 MeV. The arrows display the neutron spectra produced by the D–D reaction and the maximum energy ranges of the neutron spectra produced by the D–^{12}C and ^{12}C–D reactions.

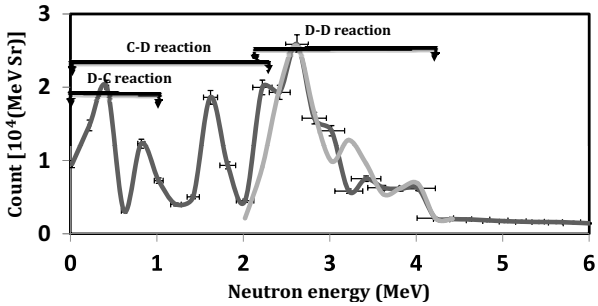

Figure 4. Comparison between the measured neutron spectra (black) and the calculated spectra for the D–D reaction by 3D Monte Carlo code (grey) at observation angle 70°. The D–D reaction can introduce an acceptable interpretation for the measured neutron spectra from 2.1 ± 0.14 MeV to 4 ± 0.28 MeV. The arrows display the neutron spectra produced by the D–D reaction and the maximum energy ranges of the neutron spectra produced by the D–^{12}C and ^{12}C–D reactions.

In this reaction a deuteron dissociates into proton and neutron by an electron with energy of 2.225 MeV or higher. The cross section of this reaction is extremely small $\sim 10\,\mu$b [26]. Besides, we must note that this mechanism is not effective in producing neutrons because electrons scatter at large angles out of the target region.

(3) *Reactions between D ions and ^{12}C ions*:

$$\mathrm{D} + {}^{12}\mathrm{C} \rightarrow {}^{13}\mathrm{N} + \mathrm{n} - 0.28\,\mathrm{MeV}, \qquad E_{\mathrm{th}} = 0.33\,\mathrm{MeV},$$

$$^{12}\mathrm{C} + \mathrm{D} \rightarrow {}^{13}\mathrm{N} + \mathrm{n} - 0.28\,\mathrm{MeV}, \qquad E_{\mathrm{th}} = 1.96\,\mathrm{MeV}.$$

As the CD2 target contains carbon, the reactions between deuterium and carbon ions are expected. The D–^{12}C reaction between accelerated D ions and target background ^{12}C ions is possible as soon as the kinetic energy of the incident D ions exceeds the reaction threshold energy (i.e. 0.33 MeV). Compared with the D–D reaction, the D–^{12}C reaction has a very high cross section. While the maximum value of the D–D reaction cross section is around 100 mb within the energy range 0–5 MeV [25, 27], that of the D–^{12}C reaction is around 250 mb within the energy range 0.33–5 MeV [28]. The reaction D–^{12}C is an endoergic reaction so that it produces neutrons with energies lower than that of the D–D reaction for the same energy of the incident D ions. In our case, the deuterium ions are accelerated up to 1.3 ± 0.22 MeV and as a result the D–^{12}C reaction will produce neutrons with energies up to 1.02 ± 0.23 MeV (equation (1)) as shown in figures 3 and 4.

Moreover, carbon ions can be accelerated to the same maximum velocity as deuterium ions [18, 29]. Therefore, the maximum energy of ^{12}C ions can be six times (i.e. 7.8 ± 1.3 MeV) that of D ions. Carbon ions that have energies $\geqslant 1.96$ MeV (the threshold energy of the ^{12}C–D reaction) can produce neutrons through the interaction with the target background D ions. As the maximum energy of the incident ^{12}C ion can reach 7.8 ± 1.3 MeV, the ^{12}C–D reaction can produce neutrons with energies up to 2.4 ± 0.39 MeV (equation (1)) as shown in figures 3 and 4. Now, it is clear that taking into account the D–^{12}C and ^{12}C–D reactions can explain the existence of the neutron spectra emitted with energies lower than the spectra of the D–D reaction.

It is known that the cross sections of the D–^{12}C and ^{12}C–D reactions are the same in the centre-of-mass system. In the laboratory system, when ^{12}C ions have the same velocity as D ions, the cross section of the ^{12}C–D reaction becomes approximately twice that of the D–^{12}C reaction [29]. The endothermic reactions such as the D–^{12}C and ^{12}C–D reactions produce neutrons with energies starting from an extremely small value (theoretically zero) extending to a maximum value determined by the maximum energy of the incident ions. The neutrons from these reactions can overlap the D–D reaction neutrons with increasing energy of the accelerated ions. For example, in the case of deuterium ions accelerated inside the target up to 3 MeV (^{12}C ions will be six times), the neutron spectra of the D–^{12}C reaction will extend to 2.7 MeV and that of the ^{12}C–D reaction will enlarge beyond 5 MeV (equation (1)). Then, these spectra will overlap the D–D reaction spectra including the 2.45 MeV neutrons. At the same time, due to their high cross sections, the D–^{12}C and ^{12}C–D reactions will strongly take part in the total neutron yield.

Unfortunately the differential cross section data of the D–^{12}C and ^{12}C–D reactions are not available. Accordingly, the produced spectra from these reactions could not be calculated for the same observation angles as the measured ones. However, the total neutron yields of the reactions D–D, D–^{12}C and ^{12}C–D have been estimated from equation (2) by using the total cross section values and the total number of the accelerated D and ^{12}C ions. The best fitting to the experimental results is obtained when the number of accelerated D ions was 2×10^{12} sr^{-1}. This means that the total number of accelerated D ions is close to 2×10^{13} and the expected total number of accelerated ^{12}C ions (50% of D ions) is around 10^{13}. The estimated total neutron yield (in the 4π space) of the D–D reaction is 9×10^5 whereas those of the D–^{12}C and ^{12}C–D reactions are 2.3×10^5 and 4.1×10^5, respectively. These results are reasonably consistent with the prediction of kinetic numerical simulations by Toupin *et al* [29].

(4) *Reactions of D ions with ^{13}C ions*:

$$\mathrm{D} + {}^{13}\mathrm{C} \rightarrow {}^{14}\mathrm{N} + \mathrm{n} + 5.32\,\mathrm{MeV}.$$

It is known that natural carbon contains 99% ^{12}C and 1% ^{13}C. For this reason, the D–^{13}C reaction can be safely neglected due

to the small amount of ^{13}C with respect to ^{12}C even though the cross section is similar to that of the D–^{12}C reaction. In addition, neutrons with energies $\geqslant$5 MeV have to be observed in the forward directions if this reaction occurs. We cannot see such neutrons and the maximum energy of the observed neutrons is 4.5 $\pm$ 0.31 MeV.

(5) *Reactions of deuterons with the chamber wall (Al)*:

$$\mathrm{D} + {}^{27}\mathrm{Al} \rightarrow {}^{24}\mathrm{Na} + 3\mathrm{p} + 2\mathrm{n} - 5.36\,\mathrm{MeV},$$
$$E_{\mathrm{th}} = 5.75\,\mathrm{MeV},$$
$$\mathrm{D} + {}^{27}\mathrm{Al} \rightarrow {}^{22}\mathrm{Na} + 3\mathrm{p} + 4\mathrm{n} - 22.51\,\mathrm{MeV},$$
$$E_{\mathrm{th}} = 24.18\,\mathrm{MeV}.$$

It is obvious from the threshold energies of these reactions that they would take place only when deuterons with energies $\geqslant$5.75 MeV are incident on the chamber wall. Such energies are much higher than the maximum acceleration energy of deuterium ions in our case (i.e. 1.3 MeV) and as a result these reactions are impossible.

(6) *Photonuclear reactions*. Photonuclear reactions were produced by the hard bremsstrahlung x-rays or γ-rays generated due to the stopping power of the relativistic electrons through the target. For CD2 targets, these reactions take place inside the target (with D and C ions) and with the chamber wall (Al) as follows:

(a) *Deuteron photo-dissociation*:

$$\gamma + \mathrm{D} \rightarrow \mathrm{P} + \mathrm{n} - 2.225\,\mathrm{MeV}, \qquad E_{\mathrm{th}} = 2.225\,\mathrm{MeV}.$$

(b) *Carbon photo-dissociation*:

$$\gamma + {}^{12}\mathrm{C} \rightarrow {}^{11}\mathrm{B} + \mathrm{n} - 18.7\,\mathrm{MeV},$$
$$E_{\mathrm{th}} = 18.7\,\mathrm{MeV},$$
$$\gamma + {}^{13}\mathrm{C} \rightarrow {}^{12}\mathrm{C} + \mathrm{n} - 4.9\,\mathrm{MeV}, \qquad E_{\mathrm{th}} = 4.9\,\mathrm{MeV}.$$

(c) *Reactions of the emitted photons with the chamber wall*:

$$\gamma + {}^{27}\mathrm{Al} \rightarrow {}^{26}\mathrm{Al} + \mathrm{n} - 13.06\,\mathrm{MeV},$$
$$E_{\mathrm{th}} = 13.06\,\mathrm{MeV},$$
$$\gamma + {}^{27}\mathrm{Al} \rightarrow {}^{25}\mathrm{Mg} + \mathrm{p} + \mathrm{n} - 19.36\,\mathrm{MeV},$$
$$E_{\mathrm{th}} = 19.36\,\mathrm{MeV}.$$

The bremsstrahlung flux due to the stopping power of the relativistic electrons inside a CD2 target is similar to that from a pure C target at the same density. For carbon, the bremsstrahlung radiation length is approximately 43 g cm^{-2} and the electron stopping power at MeV energies is about 2 MeV cm^2 g^{-1} [30]. Consequently, our target, which is 5 μm in thickness, is too thin to stop the relativistic electrons inside it. This means that the probability of producing bremsstrahlung radiation due to the stopping power of the accelerated electrons inside the target is negligible in our case. In addition, the threshold energies of all the above-mentioned reactions are high and their cross sections are very small [31–34]. Taking into account all these factors, producing neutrons from photonuclear reactions is not possible in our case.

(7) *Reactions of protons (that contaminate the target surface)*. When an ultraintense laser interacts with a solid target, protons coming from the hydrocarbon and/or water contamination on the target surface are accelerated. The accelerated protons induce nuclear reactions inside the target and with the chamber wall. For CD2 targets irradiated by ultraintense lasers, these reactions can be divided into two categories:

(a) *Reactions with deuterium and carbon ions inside the target*:

$$\mathrm{P} + {}^{2}\mathrm{H} \rightarrow \mathrm{P} + \mathrm{n} + \mathrm{P} - 2.225\,\mathrm{MeV},$$
$$E_{\mathrm{th}} = 3.34\,\mathrm{MeV},$$
$$\mathrm{P} + {}^{12}\mathrm{C} \rightarrow {}^{12}\mathrm{N} + \mathrm{n} - 18.2\,\mathrm{MeV},$$
$$E_{\mathrm{th}} = 19.72\,\mathrm{MeV}.$$

(b) *Reactions with the chamber wall (Al)*:

$$\mathrm{P} + {}^{27}\mathrm{Al} \rightarrow {}^{27}\mathrm{Si} + \mathrm{n} - 5.59\,\mathrm{MeV},$$
$$E_{\mathrm{th}} = 5.80\,\mathrm{MeV},$$
$$\mathrm{P} + {}^{27}\mathrm{Al} \rightarrow {}^{22}\mathrm{Na} + 3\mathrm{p} + 3\mathrm{n} - 20.28\,\mathrm{MeV},$$
$$E_{\mathrm{th}} = 21.03\,\mathrm{MeV},$$
$$\mathrm{P} + {}^{27}\mathrm{Al} \rightarrow {}^{24}\mathrm{Na} + 3\mathrm{p} + \mathrm{n} - 23.71\,\mathrm{MeV},$$
$$E_{\mathrm{th}} = 24.59\,\mathrm{MeV},$$
$$\mathrm{P} + {}^{27}\mathrm{Al} \rightarrow {}^{18}\mathrm{F} + 5\mathrm{p} + 5\mathrm{n} - 28.78\,\mathrm{MeV},$$
$$E_{\mathrm{th}} = 29.825\,\mathrm{MeV}.$$

As the charge to mass ratio of the proton ion is twice that of the deuterium ion, the estimated maximum energy of the accelerated proton ions would be twice that of the deuterium ions. This means that protons, in our case, can be accelerated up to 2.6 $\pm$ 0.44 MeV. The threshold energies of all the above reactions are much higher than this value and, therefore, these reactions can be safely ignored.

After this analysis of all the possible neutron producing reactions when ultraintense lasers irradiate CD2 targets, it is clear that the D–D reaction is not the only reaction producing neutrons. The D–^{12}C and ^{12}C–D reactions strongly participate in neutron production at laser intensities of the order of 10^{18} W cm^{-2} (like this work). Furthermore, under higher irradiation conditions, all the above-mentioned reactions have to be investigated.

4. Conclusion

In conclusion, we have studied in detail the neutron production process when an ultraintense laser at intensities of the order of 10^{18} W cm^{-2} focused on a CD2 target. All the possible neutron producing reactions are analysed. The measured neutron spectra and the calculated ones, by a 3D Monte Carlo code, pointed out that D–D reaction, to which neutrons are usually attributed, is not the only source of produced neutrons. Neutrons with energies lower than that produced by the D–D reaction were observed. Analysing the other possible neutron producing reactions, we found that the D–^{12}C and ^{12}C–D reactions are the sources of these neutrons. Thus, a complete explanation for the measured neutron spectra has been provided. We have to keep in mind that with increasing energy of the accelerated ions, neutron spectra produced

by the D–^{12}C and ^{12}C–D reactions can effectively overlap that produced by the D–D reaction including the 2.45 MeV neutrons. Furthermore, due to the high cross sections of the D–^{12}C and ^{12}C–D reactions, their neutron yields strongly participate in the total neutron yield. We have to recognize that many reactions, from the above-mentioned ones, will gain more importance and can effectively contribute to neutron production under higher irradiation conditions. These results have to be taken into account during the ICF experiments that use carbon-deuterated targets.

Acknowledgments

The authors are very grateful to the members of the Laser, Target and measurement Tech. in ILE, Osaka, Japan.

References

[1] Perry M.D. *et al* 1999 *Opt. Lett.* **24** 160
[2] Roth M. *et al* 2001 *Phys. Rev. Lett.* **86** 436
[3] Raloff J. 1999 *Sci. News* **156** 257
[4] Santala M.I.K. *et al* 2001 *Appl. Phys. Lett.* **78** 19
[5] Gemmel D.S. 1974 *Rev. Mod. Phys.* **46** 129
[6] de Conto J.M. 1999 *J. Phys. IV (France)* **9** 115
[7] Bichenkov V.Y., Tikhonchuk V.T. and Tolonnikov S.V. 1999 *JETP* **88** 1137
[8] Youssef A., Kodama R., Habara H., Tanaka K.A., Sentoku Y., Tampo M. and Toyama Y. 2005 *Phys. Plasmas* **12** 110703
[9] Youssef A., Kodama R. and Tampo M. 2006 *Phys. Plasmas* **13** 030701
[10] Youssef A., Kodama R. and Tampo M. 2006 *Phys. Plasmas* **13** 030702
[11] Norreys P.A. *et al* 1998 *Plasma Phys. Control. Fusion* **40** 175
[12] Pretzler G. *et al* 1998 *Phys. Rev.* E **58** 1165
[13] Kodama R. *et al* 1999 *Plasma Phys. Control. Fusion* **41** A419
[14] Disdier L. *et al* 1999 *Phys. Rev. Lett.* **82** 1454
[15] Tanaka K.A. *et al* 2000 *Phys. Plasmas* **7** 2014
[16] Habara H. *et al* 2004 *Phys. Rev.* E **69** 036407
[17] Hilscher D. *et al* 2001 *Phys. Rev.* E **64** 016414
[18] Izumi N. *et al* 2002 *Phys. Rev.* E **65** 036413
[19] Kitagawa Y. *et al* 1999 *Fusion Eng. Des.* **44** 261
[20] Lerche R.A. and Phillion D.W. 1991 *Conf. Record of the IEEE Nuclear Science Symp. and Medical Imaging Conf. (IEEE, Piscataway, NJ, 1991)* vol I, 91CH3100-5
[21] Leeper R.J. and Chang J. 1982 *IEEE Trans. Nucl. Sci.* **NS-29** 798
[22] Knoll G.F. 1999 *Radiation Detection and Measurement* 3rd edn (New York: Wiley)
[23] Halliday D. 1955 *Introductory Nuclear Physics* 2nd edn (New York: Wiley)
[24] Jackson J.D. 1998 *Classical Electrodynamics* 3rd edn (New York: Wiley) p 645 chapter 13, section 13.6
[25] Liskin H. and Paulsen A. 1973 *Nucl. Data Tables* **11** 569–619
[26] Harder D. *et al* 1970 *Phys. Lett.* B **32** 610
[27] Krauss A., Becker H.W., Trautvetter H.P., Rolfs C. and Brand K. 1987 *Nucl. Phys.* A **465** 150
[28] Michelmann R.W., Krauskopf J., Meyer J.D. and Bethge K. 1990 *Nucl. Instrum. Methods* B **51** 1
[29] Toupin C., Lefebvre E. and Bonnaud G. 2001 *Phys. Plasmas* **8** 1011
[30] Seltzer S.M. and Berger M.J. 1985 *Nucl. Instrum. Methods Phys. Res.* B **12** 95
[31] Hadjimichael E. *et al* 1987 *Phys. Rev.* C **36** 44
[32] Fultz S.C. *et al* 1966 *Phys. Rev.* **143** 790
[33] Jury J.W. *et al* 1979 *Phys. Rev.* C **19** 1684
[34] Veyssiere A. *et al* 1974 *Nucl. Phys.* A **227** 513